

# We are IntechOpen, the world's leading publisher of Open Access books Built by scientists, for scientists

6,900

Open access books available

186,000

International authors and editors

200M

Downloads

Our authors are among the

154

Countries delivered to

TOP 1%

most cited scientists

12.2%

Contributors from top 500 universities



WEB OF SCIENCE™

Selection of our books indexed in the Book Citation Index  
in Web of Science™ Core Collection (BKCI)

Interested in publishing with us?  
Contact [book.department@intechopen.com](mailto:book.department@intechopen.com)

Numbers displayed above are based on latest data collected.  
For more information visit [www.intechopen.com](http://www.intechopen.com)



# Microscopic Structure and Dynamics of Molecular Liquids and Electrolyte Solutions Confined by Carbon NanoTubes: Molecular Dynamics Simulations

Oleg N. Kalugin<sup>1</sup>, Vitaly V. Chaban<sup>1,2</sup> and Oleg V. Prezhdo<sup>2</sup>

<sup>1</sup>*V. N. Karazin Kharkiv National University,*

<sup>2</sup>*University of Rochester,*

<sup>1</sup>*Ukraine,*

<sup>2</sup>*USA*

## 1. Introduction

Carbon nanotubes (CNT) are a completely new carbon material that are expected to become typical raw material for nanotechnology, applied to such broad fields as composite materials, electronic devices, drug delivery nanocapsules, etc. (Abrahamson & Nair, 2008; Abrikosov et al., 2005; Ahmad et al., 2006; Ajayan & Zhou, 2001; Avouris, 2002; Back & Shim, 2006; Bordjiba et al., 2008; Danilov et al., 2005; Eletsii, 1997; Hilder & Hill, 2008; Z. Liu et al., 2008; F. Yang et al., 2008; X. Yang et al., 2008; Zhang et al., 2007).

One of the most interesting and promising is application of CNTs as electrode materials (Centeno et al., 2007; Janes et al., 2007; Huang et al., 2008; R. Lin et al., 2009). Nanoporous carbon exhibits excellent charge-discharge properties and a stable cyclic life. Moreover, activated composite carbon films generate high specific capacitance, laying the foundation for a new generation of double-layer super-capacitors (SC) (Endo et al., 2008; Huang, et al., 2008; Wu & Xu, 2006). CNT provides an ideal model for investigating the microscopic details of fluid transport in these nanoporous carbon structures. SC design requires polar, but aprotic solvents such as acetonitrile (AN). In spite of the great fundamental and practical importance of AN, its structural and dynamical properties inside CNTs have never been investigated yet.

The fuel cells (Li et al., 2004; Maclean & Lave, 2003), which directly transform the chemical reaction energy between hydrogen and oxygen into electric energy, are seen as the energy source of the next-generation. With their environmentally friendly and high efficiency characteristics, the cells are being researched and developed as the future energy for automobiles and as energy generation for the houses. Since the CNTs have the possibility of clearly surpassing raw materials used so far, the aspects of applying it to fuel cell electrodes is under consideration (M.L. Lin et al., 2008). The most promising fuel cells are based on methanol (MeOH, CH<sub>3</sub>OH) which is renewable and easily storable (Convert et al., 2001; Gu & Wong, 2006; Hsieh & J.Y. Lin, 2009; Hsieh et al., 2009; H.S. Liu et al, 2006; Qi et al.; 2006;

Schultz et al., 2001; Suffredini et al., 2009; C.H. Wang et al., 2007; Z. Wang et al., 2008). In view of the present large interest on the methanol behavior inside nanopores, it is highly informative to carry out MD simulation on liquid methanol confined by CNTs to elucidate an influence of CNT internal diameter on microscopic structure and dynamic (transport) properties of this alcohol.

Dimethyl sulphoxide (DMSO) is an important polar aprotic solvent, widely used in the chemical industry, biology and medicine, that dissolves both polar and nonpolar compounds (Martin & Hanthal, 1975; Yu & Quinn, 1994, 1998). Due to its distinctive property of penetrating the skin very readily, DMSO is an imprescriptible agent in medicine used as a carrier for transporting remedies into a human body. In this context, transport properties of liquid DMSO inside the biological nanoporous materials are of potential interest. From this point of view, internal space of CNTs can be considered as ideal model for investigation of DMSO behavior in the molecular-scale confined space.

From the fundamental point of view, the comparison of microscopic properties of confined molecular liquids with significantly differing kinds of molecular structure is of potential interest. The possibility to estimate and predict transport properties of these liquids inside carbon nanoporous structures forms a basis for their future nanotechnological and pharmaceutical applications together with carbon nanotubes. Speaking in a more general case, CNTs can be substituted with nanoporous carbon. Unfortunately, investigation of the confined liquids by means of direct experimental techniques is still quite a tricky task, so atomistic computer simulations are of ultimate importance.

In the present paper, the influence of spatial confinements caused by internal space of Single Walled Carbon Nanotubes (SWCNTs) and Multi Walled Carbon Nanotubes (MWCNTs) on microscopic structure and particle dynamics of the confined non-aqueous molecular liquids acetonitrile, methanol, dimethyl sulphoxide (AN, MeOH, DMSO) and infinitively diluted solutions of  $\text{Li}^+$  in MeOH and solutions of  $\text{Et}_4\text{NBF}_4$  of finite concentrations in AN are investigated conducting molecular dynamics (MD) simulations on them.

## 2. Details of molecular dynamics simulations

### 2.1 SWCNTs-based systems

A series of MD simulations of non-capped armchair SWCNTs with liquid AN, MeOH, MeOH+ $\text{Li}^+$  and DMSO located both inside and outside them have been performed. The simulated systems (Fig. 1) were implemented as square parallelepipeds with a ratio of side lengths approximately equal to the ratio of the length to the diameter of the corresponding SWCNT. The SWCNT centre-of-mass coincided with a geometrical centre of the molecular dynamics cells. The SWCNTs were surrounded by a few layers of solvent molecules (outside solvent) allowing the solvent particles to migrate both inside and outside the nanotube during the simulation. As an example, in Fig. 1 and 2 the snapshots of MD simulation cells from simulations of AN confined inside SWCNT(15,15) and the sketch of the MD cell along with SWCNT(22,22) and MeOH molecules are shown. Table 1 summarizes the designation, parameters, and some simulation details of the modeled systems. For reference purpose, the corresponding properties of bulk systems are discussed as well. For all the modeled systems, the values dielectric constant and density of the liquids were put equal to the experimental ones (Poltoratchkij, 1984).

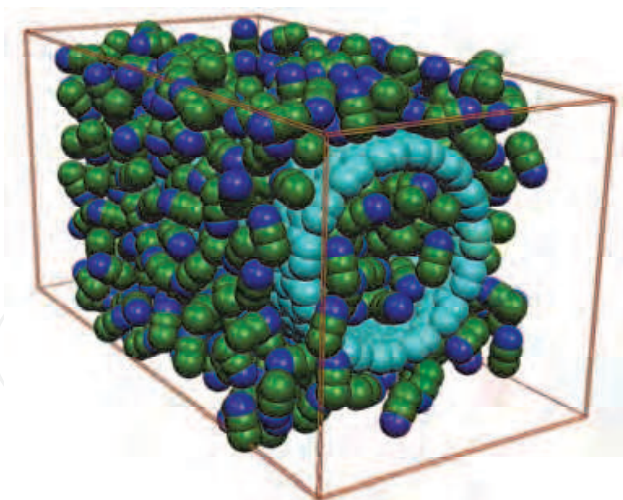


Fig. 1. Snapshots of MD simulation cells with AN confined inside SWCNT(15,15).

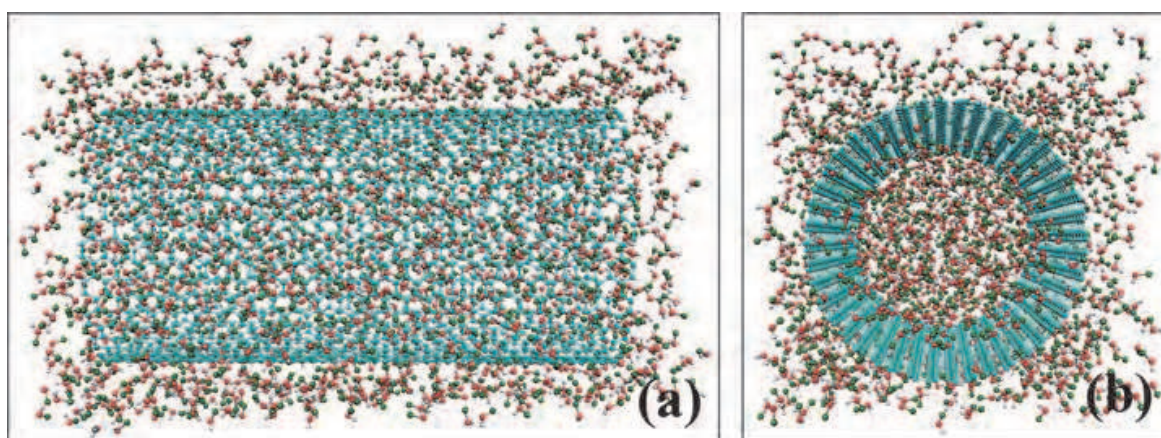


Fig. 2. Sketch of the MD cell along with SWCNT (22,22) and MeOH molecules: (a) side view, (b) cross-sectional view.

## 2.2 MWCNTs – based systems

In contrast to the previous systems, the structural and dynamic properties of the solutions of  $\text{Et}_4\text{NBF}_4$  of finite concentration in acetonitrile were modeled inside of MWCNTs without any ionic or molecular species outside. The length of the greatest edge MD cell (square parallelepiped) was chosen equal to the tube length. This, along with periodic boundary conditions in an axial direction, allows one to create a model equivalent to infinitely long nano-sized carbon channel of the cylindrical form filled by electrolyte solution. Such systems have a great practical interest for development of modern double-layer supercapacitors. For maintenance of realistic interparticle interaction potential of a solution inside of inner volume of MWCNT, a number of walls of MWCNTs was chosen equal to three in order to the total thickness of MWCNT was bigger than cut-off radius of van-der-Waals interactions in the MD cell.

The composition of the modelled systems consisting of AN molecules,  $\text{Et}_4\text{N}^+$  and  $\text{BF}_4^-$  ions ( $\text{Et}_4\text{NBF}_4$ ) and MWCNTs is presented in Table 2. Dielectric constant of the solution was taken equal to its value for pure acetonitrile, and density at 298 K was measured in our laboratory.

System	Solvent	SWCNT	SWCNT diameter, nm	SWCNT length, nm	Number of molecules	Number of ions
IA	AN	Bulk	–	–	216	0
IIA		(26,26)	3.526	7.010	1530	0
IIIA		(22,22)	2.984	6.026	887	0
IVA		(19,19)	2.577	5.042	608	0
VA		(15,15)	2.035	4.058	432	0
VIA		(11,11)	1.493	3.074	281	0
VIIA		(8,8)	1.087	2.091	216	0
IM	MeOH	Bulk	–	–	324	0
IIM		(22,22)	2.984	6.030	428	0
IIIM		(15,15)	2.035	6.030	890	0
IVM		(8,8)	1.087	6.030	1530	0
VM		Bulk			323	1 Li <sup>+</sup>
VIM		(22,22)	2.984	6.030	427	1 Li <sup>+</sup>
VIIM		(15,15)	2.035	6.030	889	1 Li <sup>+</sup>
VIIIM	(8,8)	1.087	6.030	1529	1 Li <sup>+</sup>	
ID	DMSO	Bulk	–	–	572	0
IID		(22,22)	2.984	6.030	572	0
IIID		(15,15)	2.035	6.030	918	0
IVD		(8,8)	1.087	6.030	1000	0

Table 1. Designation and some parameters of the modelled systems based on SWCNTs with AN, MeOH and DMSO.

System	MWCNT	MWCNT inner diameter, nm	Number of AN molecules	Number of electrolytes molecules	Density, kg/m <sup>3</sup>	Molarity, mol/l
IE	(15,15) (20,20) (25,25)	1.655	133	7 Et <sub>4</sub> NBF <sub>4</sub>	842.8	0.8428
IIE	(19,19) (24,24) (29,29)	2.197	236	12 Et <sub>4</sub> NBF <sub>4</sub>	842.8	0.8428
IIIE	(22,22) (27,27) (32,32)	2.604	333	17 Et <sub>4</sub> NBF <sub>4</sub>	842.8	0.8428
IVE	–	Bulk	333	17 Et <sub>4</sub> NBF <sub>4</sub>	842.8	0.8428

Table 2. Some parameters of the modelled systems based on the solutions of Et<sub>4</sub>NBF<sub>4</sub> in AN confined by MWCTNs.

As an example, the snapshot of MD simulation cell representing the system IIE is shown in Fig. 3.

### 2.3 General approach

The MD simulations of all systems were performed with a 1 fs time-step, in the NVT ensemble, with periodic boundary conditions in all directions at 298 K using Berendsen thermostat with a characteristic thermostat time equal to 100 fs. System equilibrations have been performed over 200 ps for pure solvents and 2000 ps for electrolyte solutions, and the data were collected over at least 5 runs of 500 ps and 5000 ps for molecular liquids and Et<sub>4</sub>NBF<sub>4</sub>-AN systems, respectively. The simulations have been carried out using the proprietary software package MDCNT (Molecular Dynamics inside Carbon NanoTubes) (Kalugin et al., 2006) developed by us at the Department of Inorganic Chemistry of V.N. Karazin Kharkiv National University.

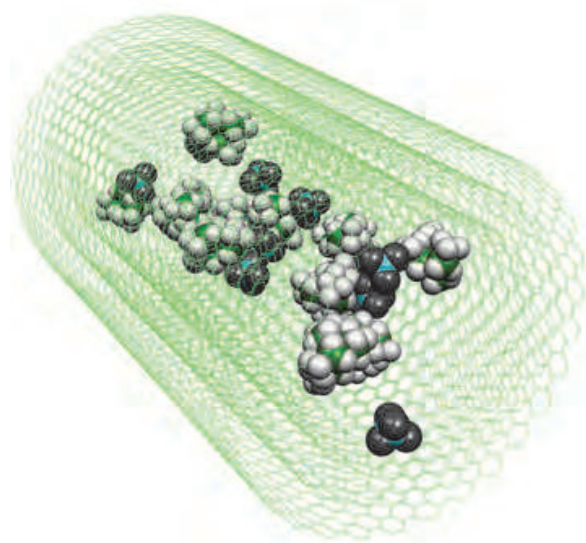


Fig. 3. Snapshots of MD simulation cell representing the system IIE. The AN molecules are not shown.

The site-site interactions between all atom pairs in the system are given by the sum of Lennard-Jones (LJ) 12-6 and Coulomb potentials,

$$U(r_{ij}) = 4\varepsilon_{ij} \left[ \left( \frac{\sigma_{ij}}{r_{ij}} \right)^{12} - \left( \frac{\sigma_{ij}}{r_{ij}} \right)^6 \right] + \frac{q_i q_j e^2}{4\pi\varepsilon_0 r_{ij}} \quad (1)$$

where  $\varepsilon_{ij}$  and  $\sigma_{ij}$  are the LJ parameters between sites  $i$  and  $j$  of distinct molecules,  $q_i$  is the partial charge on site  $i$ , and  $r$  is the site-site separation. Cross interactions were obtained from Lorentz-Berthelot combining rules,  $\varepsilon_{ij} = \sqrt{\varepsilon_{ii}\varepsilon_{jj}}$  and  $\sigma_{ij} = (\sigma_{ii} + \sigma_{jj})/2$ . Shifted force potential was employed for the LJ part of the potential, whereas the reaction field method was used to calculate the long-range Coulombic part. In this work we used the well-tested force field models for solvent (the three-site rigid A3 (Mountain, 1997) for AN, the three-site rigid H1 (Haughney et al. 1987) for MeOH, and the four-site rigid VG (H. Liu et al., 1995) for DMSO) which imply the intermolecular interactions to be a sum of Coulomb and Lennard-Jones (LJ) (12, 6) potentials, rigid bonds and fixed angles in the solvent molecules. Usage of the force field model with rigid bond and angle values is justified by the different time

scales of intra- and intermolecular motions in the case of these liquids. The techniques of reaction field and shifted force were applied to Coulomb and LJ (12, 6) interactions, respectively.

LJ-parameters for  $\text{Li}^+$  were restored from the van-der-Waals parameters (Peng et al., 1997) according to the procedure described earlier (Kalugin et al., 2003) and already applied in our previous works.

The force-field of the CNT carbon atoms was taken to be purely LJ (Van Gunsteren et al., 1996). The geometrical parameters of ideal armchair CNTs were generated by the proprietary algorithm (Kalugin et al., 2006) with the length of carbon-carbon bond equal to 0.1421 nm. The carbon atoms of the CNTs were held fixed during the MD simulations. The CNT was assumed to be rigid with a fixed carbon-carbon bond length equal to 0.1421 nm. Our previous test simulations have shown that the effect of carbon nanotube flexibility is not critical for the discussed properties of the confined molecules (Chaban et al., 2010a). All the potential parameters used in the present MD simulations are enumerated in Table 3.

Particle	Geometry	Site	$\sigma_{ii}$ , nm	$\epsilon_{ii}$ , kJ/mol	$q_i$ (e)
CNT	$r_{\text{CC}} = 0.1421$ nm	C	0.33611	0.405868	0
AN	$r_{\text{CN}} = 0.117$ nm, $r_{\text{CMe}} = 0.146$ nm, $\angle \text{MeCN} = 180^\circ$	Me	0.36	1.588	+0.269
		C	0.34	0.416	+0.129
		N	0.33	0.129	-0.398
MeOH	$r_{\text{OH}_o} = 0.095$ nm, $r_{\text{OMe}} = 0.142$ nm, $\angle \text{H}_o\text{OMe} = 108.53^\circ$	H <sub>o</sub>	0	0	+0.431
		O	0.3083	0.7312	-0.728
		Me	0.3861	0.7579	+0.297
DMSO	$r_{\text{SO}} = 0.153$ nm, $r_{\text{SMe}} = 0.180$ nm, $\angle \text{OSMe} = 106.75^\circ$ , $\angle \text{MeSMe} = 97.4^\circ$	S	0.356	1.29699	+0.139
		O	0.263	1.7154	-0.459
		Me	0.366	0.9414	+0.160
$\text{Li}^+$	-	Li	0.0826	26.158	+1
$\text{BF}_4^-$	tetrahedron: $r_{\text{BF}} = 0.139$ nm, $r_{\text{FF}} = 2.27$ nm	B	0	0	+0.9756
		F	0.30	0.2845	-0.4939
$\text{Et}_4\text{N}^+$ ( $\text{D}_{2d}$ symmetry)	(Kalugin et al., 2005)	C <sub>1</sub>	0.391992	0.48959	+0.03423
		C <sub>2</sub>	0.3875	0.73227	-0.28586
		H <sub>1</sub>	0	0	+0.08854
		H <sub>2</sub>	0	0	+0.10958
		N	0	0	-0.01667

Table 3. The potential parameters for interacting sites of the AN, MeOH and DMSO molecules,  $\text{Li}^+$ ,  $\text{BF}_4^-$ ,  $\text{Et}_4\text{N}^+$  ions and CNT. "Me" stands for the methyl group as united atom (site).

## 2.4 Simulated properties

Keeping in mind that there should be specific structure patterns in the cylindrical confined area, we proposed the single-atom distribution functions,  $P_\alpha(r, z)$ , of cylindrical symmetry

(Fig. 4). The cylindrical distribution functions (CDF) is defined as (Chaban et al., 2009, Chaban & Kalugin, 2010)

$$P_{\alpha}(r, z) = \rho_{\alpha}(r, z) / \langle \rho_{\alpha} \rangle^{\text{inside CNT}} \quad (2)$$

where  $\rho_{\alpha}(r, z)$  and  $\langle \rho_{\alpha} \rangle^{\text{inside CNT}}$  are the local and mean atomic density of  $\alpha$  species, respectively, inside of the SWCNT (Fig. 4).

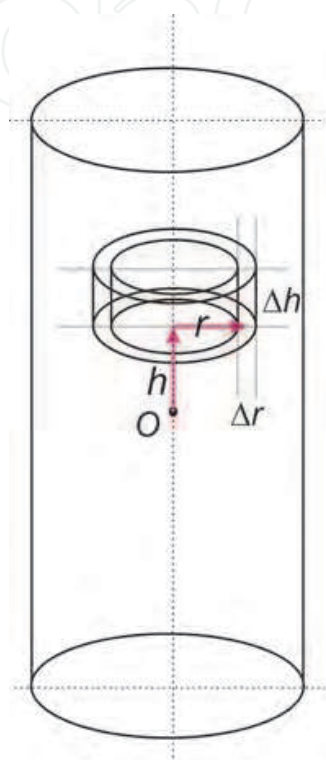


Fig. 4. The definition of the cylindrical distribution functions  $P_{\alpha}(r, z)$  (CDF).

The local densities,  $\rho_{\alpha}(r, z)$ , were calculated by dividing the confined (by the SWCNT) space into a number of slices in axial ( $z$ ) direction along the axis of the SWCNT (with a step of 0.02 nm) and a number of cylindrical shells in radial ( $r$ ) direction perpendicular to axial one (with the same step) and then taking the statistical average for the local density for each slice or shell.

To examine the re-orientational dynamics of solvent molecules inside CNTs, we evaluate the re-orientational autocorrelation functions (ACFs) of the unit vector  $\mathbf{u}$  along the molecular dipole  $\boldsymbol{\mu}$ ,

$$C_{\mu\mu}(t) = \langle \mathbf{u}(0) \cdot \mathbf{u}(t) \rangle / \langle \mathbf{u}(0) \cdot \mathbf{u}(0) \rangle \quad (3)$$

The translational self-diffusion coefficients (SDC) were derived from velocity autocorrelation functions via the Green-Kubo equation,

$$D = \lim_{t \rightarrow \infty} \frac{1}{3} \int_0^t \langle \mathbf{v}(0) \mathbf{v}(t) \rangle dt \quad (4)$$

### 3. Results and discussion

#### 3.1 AN based systems in SWCNTs

The solvent structure of AN inside SWCNTs was analyzed by computing the cylindrical distribution function  $P_{\alpha}(r, z)$  of the atomic density along the CNT axial ( $z$ ) and radial ( $r$ ) directions. Figure 5 shows two examples of the distributions of nitrogen atomic density of AN molecules confined inside the (15,15) and (19,19) armchair CNTs with the internal diameters of 1.655 nm and 2.197 nm, respectively. The same oscillatory behavior of the atomic density along the radial direction was observed for all CNTs and all AN interacting sites, including N, C and  $\text{CH}_3$ . The atomic density is maximal near the CNT wall, where molecular correlations are reinforced by the space confinement. The second maximum in the atomic density is seen about 0.35 nm after the first maximum. The height of the second maximum is  $\sim 1.5$  times smaller than the height of the first maximum. This trend was seen in all cases. At distances larger than 0.7 nm from the CNT wall the confinement effects can be neglected.

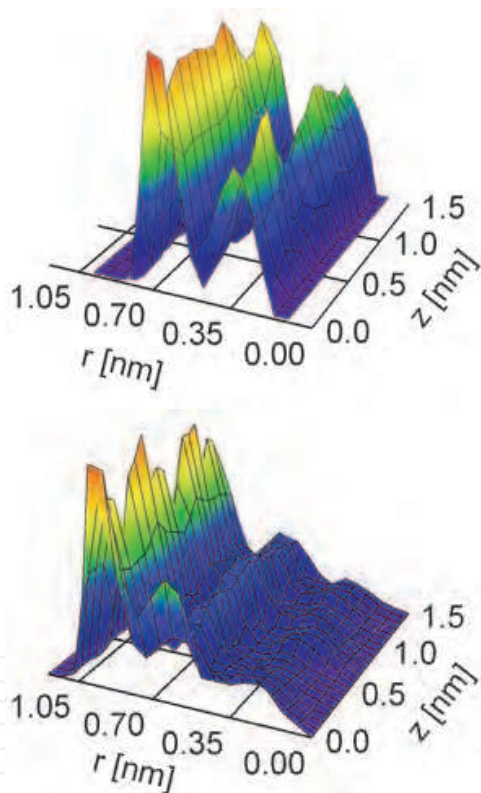


Fig. 5. Cylindrical distribution functions of nitrogen atomic density inside of CNTs (15,15) (top) (19,19) (bottom). The point (0, 0) on the each graph corresponds to the geometrical centre of the SWCNT.

One can expect that the spatial confinement of the AN molecules at distances shorter than 0.7 nm from the CNT wall should have an important impact on the solvent dynamical and transport properties. The confinement effect is seen with both the re-orientation dynamics and the diffusion coefficient. These types of motion are slowed down inside CNTs. The diffusion shows a uniform dependence on the CNT diameter, while the re-orientation exhibits strong anomalies in the CNTs whose radii are less than 0.7 nm, as elucidated below.

In order to examine the orientation dynamics of the AN molecules inside CNTs, we evaluated the orientation autocorrelation function (ACF) of the unit vector  $\mathbf{u}$  along the direction of the molecular dipole  $\boldsymbol{\mu}$ ,  $C_{\mu\mu}(t)$ . The long-time behavior of  $C_{\mu\mu}(t)$  extending beyond 2 ps is well described by a single exponential decay:  $\ln C_{\mu\mu}(t) = \text{const} - t/\tau_{\mu}$ . The corresponding orientation relaxation times,  $\tau_{\mu}$ , calculated using the least squares method from the slopes of  $\ln C_{\mu\mu}(t)$  at times between 2 and 10 ps are summarized in Table 4. The re-orientation dynamics of AN molecules inside CNTs is drastically slower than in bulk liquid. The orientation relaxation times significantly exceed the bulk value and increase with decreasing CNT diameter. A uniform behavior is seen with the nanotubes from (26,26) to (11,11), whose diameters are more than twice larger than the 0.7 nm confinement distance, discussed above. The orientation relaxation time of AN inside the (11,11) CNT, whose diameter is 1.1 nm, jumps to an extremely large value of 102 ps. Surprisingly, the relaxation time for the (8,8) tube with diameter of only 0.7 nm is quite small  $\tau_{\mu} = 18.1$  ps, and is much closer to that of the (15,15) tube,  $\tau_{\mu} = 11.9$  ps, than the (11,11) tube, even though the spatial confinement effects should be strongest in the (8,8) CNT.

System	CNT inner diameter, nm	AN self-diffusion coefficient, $D \cdot 10^9$ , $\text{m}^2\text{s}^{-1}$	AN orientation relaxation time, $\tau_{\mu}$ , ps
IA	-	$3.240 \pm 0.004$	3.9
IIA	3.526	$2.52 \pm 0.05$	7.9
IIIA	2.604	$2.27 \pm 0.05$	9.0
IVA	2.197	$2.03 \pm 0.12$	9.1
VA	1.655	$1.69 \pm 0.12$	11.9
VIA	1.113	$1.09 \pm 0.22$	102
VIIA	0.707	$0.76 \pm 0.07$	18.1

Table 4. System parameters and dynamic properties of AN molecules confined by SWCNTs.

Translational diffusion of AN inside CNTs is of great importance to a variety of applications. The self-diffusion coefficient  $D$  was calculated by the Green-Kubo formula. In order to avoid the open-end boundary effects, only AN molecules located more than one molecule diameter (0.6 nm) away from the nanotube ends were used to calculate  $D$ . The values reported in Table 2 clearly show that the diffusion coefficient of AN inside CNTs decreases with decreasing CNT diameter. The change between bulk and the 1nm (8,8) CNT is a factor of 4. The behavior of the translational diffusion coefficient is uniform, in contrast to the corresponding variation in the orientation relaxation time, Table 1. This result is very important for such practical applications as double-layer SC, which require steady solvent diffusion inside nanoporous carbon of varying pore-diameter distributions. The spatial confinement influences the translation motion to a lesser extent than the rotational motion, as follows from data reported in Table 4.

Optimization and development of electrochemical devices based on nanoporous carbon requires an analytic expression for the self-diffusion coefficient of a liquid inside the nanopores of arbitrary diameter and length. In the absence of a general theory of fluid diffusion in porous materials, we extended the recently proposed description of liquid transport under steric confinement of a solid matrix (Sevriugin et al., 2003) and obtained a

simple analytic expression for the observed trend in the diffusion coefficient (Kalugin et al., 2008), as described below.

Reference (Sevriugin et al., 2003) shows that self-diffusion of a liquid in a heterogeneous system is decreased relative to the pure liquid according to

$$D = D_0 \exp(-P_{st}) \quad (5)$$

where  $D_0$  is the bulk self-diffusion coefficient, and  $P_{st}$  is the probability of steric restrictions imposed on a particle of a fluid by the surrounding matrix. The probability  $P_{st}$  is determined by the space distribution of these steric constraints or, in the simplest case, by the confinement geometry.

Consider a liquid molecule that diffuses distance  $\Lambda$  and collides with a CNT wall, see insert in Fig. 6. Collisions occur when the molecule is close to the CNT wall and moves towards the wall. The thickness of the solvent layer that is sufficiently close to the wall to produce a collision can be estimated by the mean-free path of diffusion  $d_m$ . The directionality of the molecular motion is accounted for by the following average

$$\langle \Lambda \rangle = \int \Lambda d\Omega / \int d\Omega \quad \langle \Lambda \rangle = \int \Lambda d\Omega / \int d\Omega \quad (6)$$

in which the integration is performed over the solid angle that is directed towards the CNT wall.

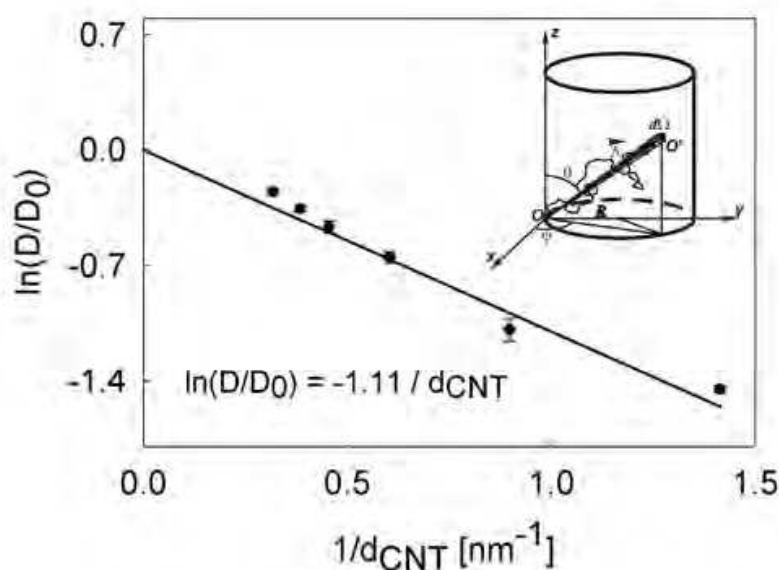


Fig. 6. Relative AN self-diffusion coefficient as a function of CNT inverse diameter. Inset: Diffusion path of a particle inside a CNT.

Geometric considerations lead to

$$\langle \Lambda \rangle \approx 0.64d \quad (7)$$

where  $d$  is the internal diameter of the CNT. The probability that the motion of the diffusing particle will be impeded by a collision with the wall is given by the ratio  $d_m / \langle \Lambda \rangle$ . Then, the expression (2) for self-diffusion coefficient in the confined geometry becomes

$$D = D_0 \exp(-d_m / 0.64d) \quad (8)$$

or, explicitly inserting the value of the mean-free diffusion path for bulk AN,  $d_m=0.65$  nm:

$$D = D_0 \exp(-1.01 / d) \quad (9)$$

Figure 6 demonstrates good agreement between this simple theoretical expression and the results of the MD simulation, given by the filled circles.

### 3.2 MeOH based systems in SWCNTs

To examine a long-range structure of a liquid methanol inside the SWCNTs, we have calculated the cylindrical distribution function  $P_\alpha(r, z)$  of the atomic density along the CNT axial ( $z$ ) and radial ( $r$ ) directions ( $\alpha$  - any site of MeOH or  $\text{Li}^+$ ) of cylindrical symmetry. Contour plots of cylindrical distribution functions  $P_\alpha(r, z)$  for the hydrogen ( $\alpha = \text{H}$ ) and oxygen ( $\alpha = \text{O}$ ) atoms of MeOH molecules inside the SWCNT (8,8), SWCNT (15,15) and SWCNT (22,22) are plotted in Fig. 7. Cylindrical atomic density distribution (Fig. 7) of MeOH confined in the CNTs demonstrates the series of intertransient maxima oriented at an angle of  $\sim 30^\circ$  with respect to the CNT axes. It is interesting to note a similar character of  $P_{\text{H}}(r, z)$  and  $P_{\text{O}}(r, z)$  distributions, that evidently indicates the chain-like hydrogen bond network in confined methanol. It should be also stressed, that CNT diameter influences the

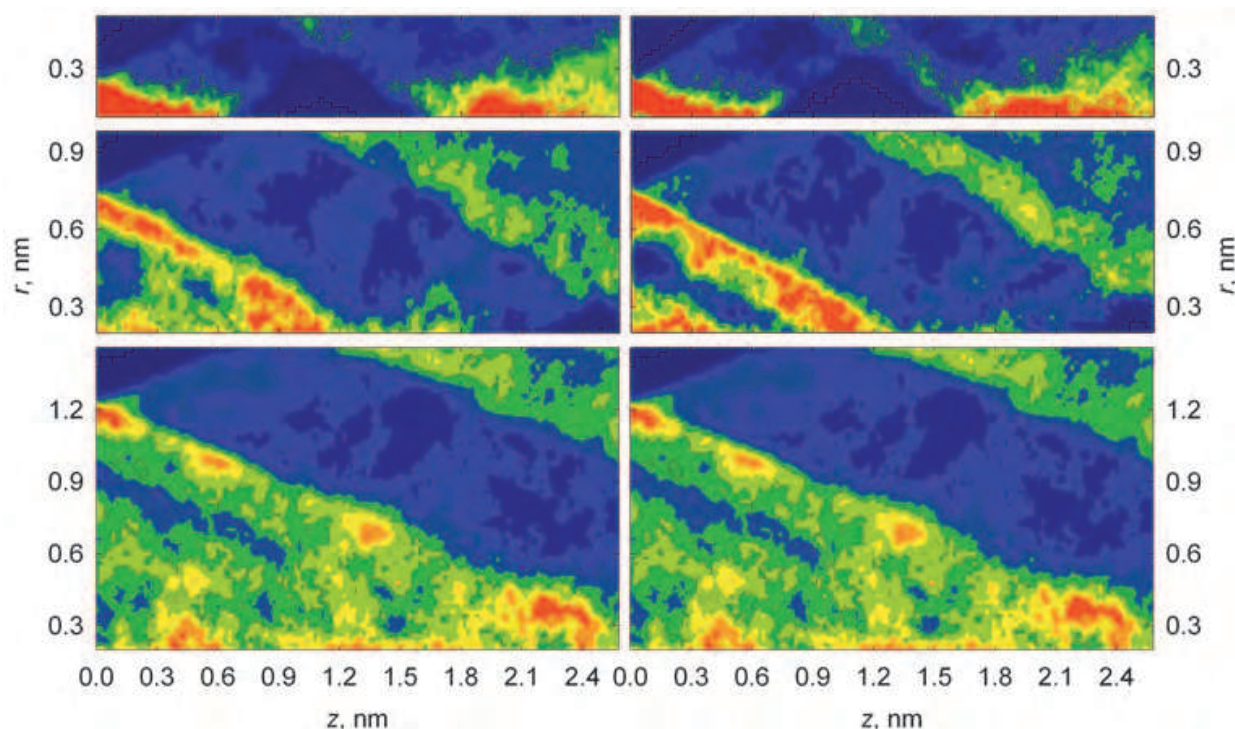


Fig. 7. Contour plots of cylindrical distribution functions  $P_\alpha(r, z)$  for the hydrogen ( $\alpha = \text{H}$ ) (left) and oxygen ( $\alpha = \text{O}$ ) (right) atoms of MeOH molecules inside the SWCNT (8,8) (top), SWCNT (15,15) (middle), and SWCNT (22,22) (bottom) derived from MD simulations on systems IIM-IVM. The point (0, 0) on the each graph corresponds to the geometrical centre of the SWCNT.

intensity of density distribution functions, but in general form of density anisotropy. These observations allow us to make a conclusion about layered long-range structure of methanol with helix-like distribution of H-bonds inside the CNTs.

The mentioned above conclusion about layered structure in liquid methanol inside the CNT is completely confirmed by instantaneous configuration of the methanol molecules inside the SWCNT (15,15) (Fig. 8). The molecular helix-like chains formed by the hydrogen-bonded MeOH molecules inside the CNTs are clearly observed.

Bearing in mind the discussed above changes in long-range structure of liquid MeOH driven by CNTs, it is interesting to identify the CNT influence on infinitely diluted solution of  $\text{Li}^+$ . In the present study, we simulated the configurations when  $\text{Li}^+$  has already gone into the CNT at maximum depth (3 nm far from any end of the CNT) and is initially equidistant from the CNT walls. Cylindrical distribution function for  $\text{Li}^+$ ,  $P_{\text{Li}}(r, z)$ , shows the permanent location of the cation around its initial position ( $r = 0, z = 0$ ). The mentioned deviation from the centre point is the same inside all the investigated CNTs and does not depend on the CNT diameter.

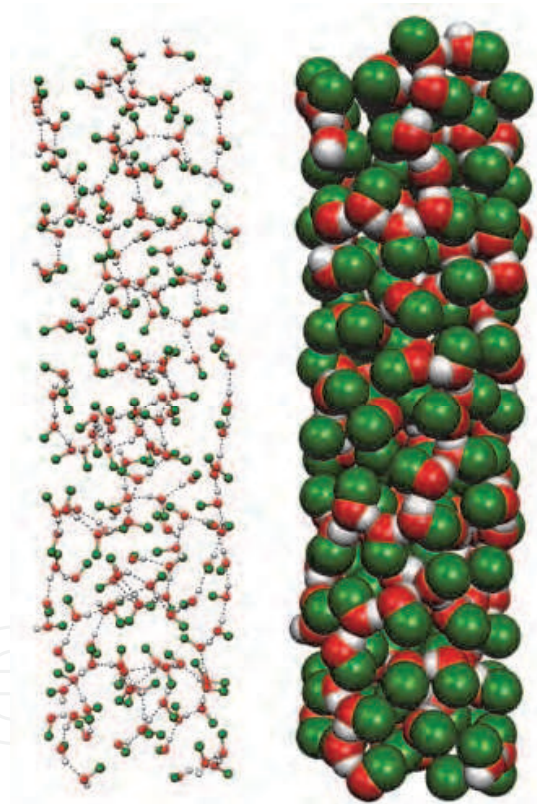


Fig. 8. Instantaneous configuration of the methanol molecules inside the SWCNT (15,15) ( $d_{\text{CNT}}=2.984$  nm) at 298 K from MD simulation on system IIM in “balls and sticks” (left) and “spacefill” (right) formats. H-bonds between MeOH molecules are indicated by dashed lines. The helix nature of the H-bond network is clearly seen.

To examine the re-orientational dynamics of the MeOH molecules inside CNTs, we evaluate the re-orientational autocorrelation functions (ACFs) of the unit vector  $u$  along the molecular dipole  $\mu$ ,  $C_{\mu\mu}(t)$ . The long time ( $t > 4$  ps) behavior of  $C_{\mu\mu}(t)$  is well described by single exponent  $\ln C_{\mu\mu}(t) = \text{const} - t/\tau_{\mu}$ . The corresponding re-orientational relaxation times,

$\tau_{\mu}$ , calculated from the slopes of  $\ln C_{\mu\mu}(t)$  (by using least squares method) at long times ( $4 \leq t \leq 10$  ps) are summarized in Table 5. It is interesting to note that the re-orientational relaxation times of MeOH molecules inside the CNTs significantly exceed the corresponding value for the bulk solvent and increase with the CNT diameter decrease. For example, inside the SWCNT (8,8),  $\tau_{\mu}$  increases more than two times in comparison with bulk.

Self-diffusion coefficients,  $D$ , of the centre of mass of MeOH molecules and lithium-ion were calculated from the velocity autocorrelation functions via the Green-Kubo relation.

The resulting  $D_{\text{MeOH}}$  and  $D_{\text{Li}^+}$  values for all the simulated systems are summarized in Table 5. The diffusion coefficients of MeOH molecules confined by CNTs are noticeably lower as compared with bulk and for the SWCNT (8,8)  $D_{\text{MeOH}}$  value is about two times lower than that without space restrictions. At the same time, diffusion coefficients of MeOH molecules depend slightly on CNT diameter,  $d_{\text{CNT}}$ . Only  $0.35 \cdot 10^{-9} \text{ m}^2 \text{ s}^{-1}$  grows in  $D_{\text{MeOH}}$  value occurs when  $d_{\text{CNT}}$  increases by a factor of three (from 1.087 nm to 2.984 nm). It allows us to conclude that the average diffusion coefficient of MeOH inside the CNT of a given diameter is sharply decreased by the first layer of parietal solvent molecules which lose one of their degrees of freedom and the structure of this layer is reinforced in the maximally possible way inside the CNT. This conclusion is in complete agreement with the H-bond structure of confined MeOH already discussed. Diffusion coefficients slowdown inside the CNTs is an important feature of the direct methanol fuel cells.

In contrast to the methanol diffusion coefficient, the decrease in  $D_{\text{Li}^+}$  values with decreasing  $d_{\text{CNT}}$  is insignificant (Table 5). This is probably caused by a location of lithium ion along with its stable solvation shell far from the internal CNT wall where the solvent dynamics is not affected sufficiently by the space restrictions.

System	$D_{\text{MeOH}} 10^9, \text{ m}^2 \text{ s}^{-1}$	$\tau_{\mu}, \text{ ps}$	System	$D_{\text{Li}^+} 10^9, \text{ m}^2 \text{ s}^{-1}$
IM	$2.16 \pm 0.02$	12	VM	$0.53 \pm 0.07$
IIM	$1.30 \pm 0.02$	18	VIM	$0.50 \pm 0.06$
IIIM	$1.25 \pm 0.06$	23	VIIM	$0.46 \pm 0.07$
IIVM	$0.95 \pm 0.06$	28	VIIIM	$0.41 \pm 0.07$

Table 5. The self-diffusion coefficients and microscopic dipole relaxation times,  $\tau_{\mu}$ , of the methanol molecules from MD simulations of the systems IM-IVM and self-diffusion coefficients of the lithium ion from MD simulations of the systems VM-VIIIM.

### 3.3 DMSO-based systems in SWCNTs

In order to clarify a long-range structure of the confined DMSO we have also analyzed the cylindrical distribution functions  $P_{\alpha}(r, z)$ . The CDFs  $P_{\text{O}}(r, z)$  of the oxygen atoms of DMSO inside all the investigated SWCNTs are shown in Fig. 9.

The highest atomic density is observed near the inner wall of SWCNT. It indicates the particular reinforcements of molecular interactions and the increase of molecules ordering at the distances  $\sim 0.5$  nm and less from the carbon atoms. That distances correspond to the first liquid layer from the wall. Inside the smallest SWCNT (8, 8), the above tendency can not be observed because all the confined DMSO molecules are located near the SWCNT inner wall (see Fig. 9).

On contrary to the acetonitrile and methanol confined by SWCNTs, no special long-range pattern in the case of DMSO is observed. Inside the SWCNT (22,22) one can identify low grade second layer of the solvent molecules at the distances ca. 0.7-0.8 nm from the SWCNT inner wall. Low sensitivity of DMSO to the presence of the SWCNT can be explained by the strong spatial correlations between the DMSO molecules due to anti-parallel alignment of their dipole moments. It appears that anisotropic dipole-dipole intermolecular interactions, that specify the structure of DMSO in liquid phase, are more powerful as compare with solvophobic interactions of the solvent molecules with carbon atoms of the SWCNT. Nevertheless, the space confinements given by the SWCNT inner wall promote these dipole-dipole correlations, but such reinforcement can not cover more then one molecular layer due to the short-range character of the dipole correlations in the liquid DMSO.

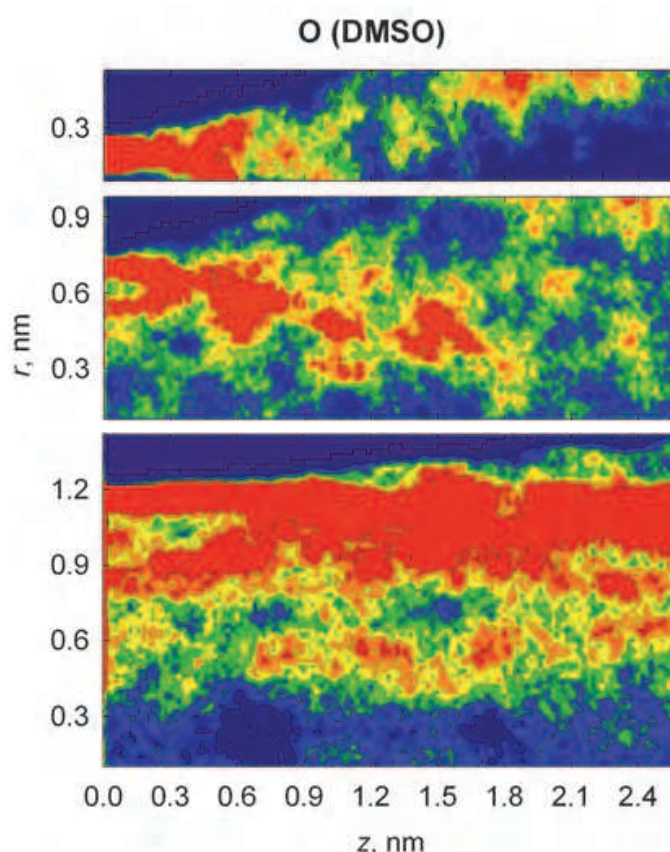


Fig. 9. Contour plots of cylindrical distribution functions,  $P_{\alpha}(r, z)$ , for Oxygen atoms of DMSO inside the SWCNTs (8, 8), (15, 15) and (22, 22) in the top, middle and bottom, respectively derived from MD simulations. The point (0, 0) on the each graph corresponds to the geometrical centre of the SWCNT.

The self diffusion coefficients (SDCs) derived from VACFs are  $0.4 \pm 0.1$ ,  $0.56 \pm 0.05$ ,  $0.62 \pm 0.05$ ,  $1.06 \pm 0.05$  ( $\times 10^{-9}$  m<sup>2</sup>/s) for SWCNTs (8, 8), (15, 15), (22, 22) and bulk, respectively. The simulated SDCs are well correlated with a value of SWCNT diameter. Performing a complex analysis of the SDCs of DMSO inside the SWCNTs against bulk value together with CDFs,  $P_{\alpha}(r, z)$ , one can assume that the general slowdown of DMSO SDCs in the case of SWCNTs is defined by the fraction of DMSO molecules in the first layer near the inner wall of the nanotube.

### 3.4 Acetonitrile solutions of Et<sub>4</sub>NBF<sub>4</sub> in MWCNTs

In the Et<sub>4</sub>NBF<sub>4</sub> solutions in AN both in the bulk phase and in confinements the wide distribution of the ionic clusters size is found (Fig. 10). The average cluster size (a number of cations Et<sub>4</sub>N<sup>+</sup> and anions BF<sub>4</sub><sup>-</sup> consisting a cluster) slightly increase from 8.4 to 12.2 as the inner diameter of MWCNTs decreases from the infinity (bulk solvent) to 1.655 nm.

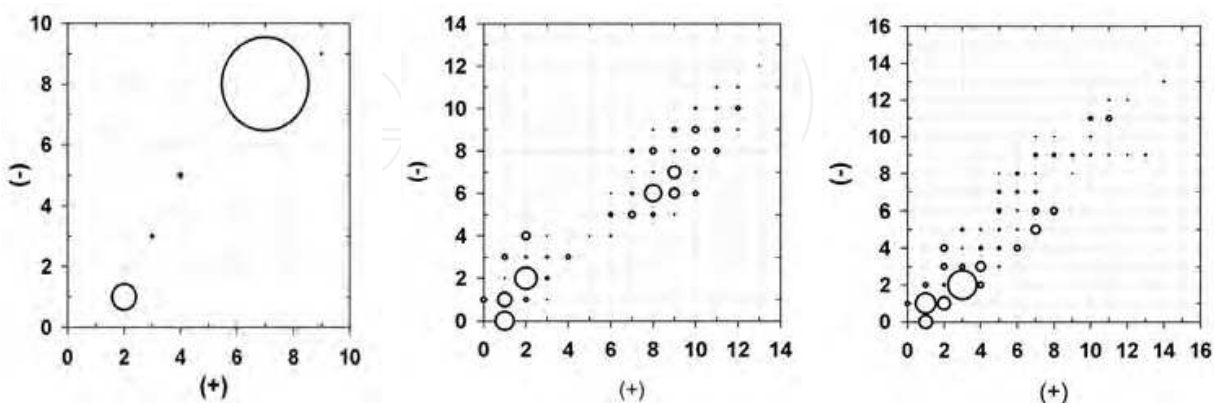


Fig. 10. Distribution of the cluster sizes for the systems IE (left), IIE (middle) and IVE (right). (+) and (-) stand for the Et<sub>4</sub>N<sup>+</sup> and BF<sub>4</sub><sup>-</sup> ions, respectively. Diameter of the circles reflects a relative probability of the formation of the corresponding cluster.

It is clarified that dynamical properties of electrolyte solutions confined by carbon nanotube are defined by two general factors: geometry of confinements and ionic subsystem structure of confined solution. Translational diffusion of AN and ions of Et<sub>4</sub>NBF<sub>4</sub> inside MWCNTs is of great importance for improvement of super capacitors. The self-diffusion coefficients  $D$  were calculated by the Green-Kubo formula and listed in Table 6.

System	MWCNT inner diameter, nm	$D(\text{AN}) 10^9, \text{m}^2 \text{s}^{-1}$	$D(\text{Et}_4\text{N}^+)10^9, \text{m}^2 \text{s}^{-1}$	$D(\text{BF}_4^-) 10^9, \text{m}^2 \text{s}^{-1}$
IE	1.655	0.63	0.25	0.29
IIE	2.197	0.74	0.28	0.35
IIIE	2.604	0.87	0.34	0.40
IVE	bulk	2.20	0.81	0.93

Table 6. Self-diffusion coefficients of the acetonitrile and ions of Et<sub>4</sub>NBF<sub>4</sub> solutions in AN from MD simulations of the systems IE-IVE.

The values reported in Table 6 clearly show that the diffusion coefficient of AN and ions inside MWCNTs decreases with decreasing internal diameter of CNT. It should be note that slowdown of ions SDCs inside of MWCNTs is not as drastic as one would expect. This is very important for optimization of pore size of the carbon nanomaterials used for the development of the modern double-layer super-capacitors.

## 4. Conclusion

To recapitulate, we elucidated the details of structure, re-orientational dynamics and translational diffusion of AN confined inside CNTs with diameters ranging from 1 nm to 3.5

nm. The geometric confinement creates a strong periodic pattern in the AN structure near the CNT wall, with the persistence length of 0.7 nm. The orientation relaxation time increases with decreasing CNT diameter and shows a highly non-uniform behavior for small CNTs, associated with specific solvent structures in the tightly confined spaces. The translational diffusion coefficient changes continuously with decreasing CNT diameter, even for the smallest CNTs. The observed dependence of the diffusion coefficient on the CNT size was described analytically with a simple model, which can be applied for optimization of electrochemical devices based on nanoporous carbon.

It was revealed that although local order of MeOH does not differ from bulk, long-range structure is helix-like near the inner CNT walls. Whereas the mechanism of hindered translations of the MeOH molecules and  $\text{Li}^+$  confined in the CNTs does not differ from bulk, translational mobility of MeOH molecules is noticeably lower than in bulk ones due to the translation self-diffusion slowdown within the first layers of the parietal solvent molecules. In contrast to MeOH, decrease of translational self-diffusion coefficients of  $\text{Li}^+$ , located along the CNT axis, is insignificant.

As it follows from the results of the performed molecular dynamics simulations on liquid dimethyl sulfoxide confined by single-walled carbon nanotubes at 298 K, the local order of DMSO analyzed in terms of site-site intermolecular radial distribution functions is similar to that in the bulk except the case with the smallest SWCNT (8, 8). Meanwhile, the microscopic structure of the confined DMSO expressed in terms of cylindrical distribution functions demonstrates well pronounced changes in a local atomic density in the vicinity of the inner wall of the SWCNT.

The translational self-diffusion coefficients of the centre-of-mass of the DMSO molecules are lower by a factor of 2-3 than bulk ones and are evidently correlated with a value of the SWCNT diameter. It is shown that the slowdown of self-diffusion coefficient of DMSO confined in the SWCNTs is reduced by the first layer of DMSO molecules close to the SWCNT wall, and this is caused by the reinforcement of the dipole-dipole correlations among DMSO molecules. The SDCs of DMSO inside of the SWCNTs are of interest for its transportation through SWCNT-based capsules for drug delivery. Based on the re-orientational dynamics of liquid DMSO in confinements analysis, it was shown that cryoprotective properties of DMSO are stipulated by the considerable growth of microscopic relaxation times in the presence of spatial confinements.

The adequacy of analytical model of rectilinear dependence of reduced diffusion coefficient logarithm on the inverse diameter of CNT for AN, the solvent without specific intermolecular interactions, was demonstrated.

On the base of self-diffusion coefficients of  $\text{Et}_4\text{N}^+$  and  $\text{BF}_4^-$  inside the CNT considerable decrease carbon nanomaterials with effective diameters of up to 3 nm are suggested as an electrode material for modern electrochemical double-layer supercapacitors.

## 5. Acknowledgements

The authors acknowledge computational support of the Ukrainian-American Laboratory in Computational Chemistry established between Kharkiv, Ukraine and Jackson, MS, U.S.A. The funding was provided in part by grants from the National Science Foundation, CHE-0701517, and Petroleum Research Fund of the American Chemical Society, 46772-AC6. V. V. C. acknowledges the funding from Fund for Fundamental Studies of V. N. Karazin Kharkiv

National University (grants # 0107V000666 and #0109U001426). O. N. K. acknowledges Yury Sapronov's Kharkiv City charitable fund for the financial support of this investigation.

## 6. References

- Abrahamson, J.T., Nair, N. (2008). Modelling the increase in anisotropic reaction rates in metal nanoparticle oxidation using carbon nanotubes as thermal conduits. *Nanotechnology*, Vol. 19, No. 19, (April 2008), pp. (195701.1-195701.8), ISSN 0957-4484.
- Abrikosov, A.A., Livanov, D.V., & Varlamov, A.A. (2005). Electronic spectrum and tunneling properties of multiwall carbon nanotubes. *Physical Review B*, Vol. 71, No. 16, (April 2005), pp. (165423.1-165423.8), ISSN 1089-5647.
- Ahmad, K., Pan, W., & Shi, S.L. (2006). Electrical conductivity and dielectric properties of multiwalled carbon nanotube and alumina composites. *Applied Physics Letters*, Vol. 89, No. 17, (September 2006), pp. (133122.1-133122.3), ISSN 0003-6951.
- Ajayan, P.M., Zhou, O.Z. (2001). Applications of carbon nanotubes, In: *Carbon Nanotubes, Topics in Applied Physics, Vol. 80*, M. S. Dresselhaus, G. Dresselhaus & Ph. Avouris (Eds.), pp. (391-425), Springer, ISBN 978-3-540-41086-7, Berlin, Heidelberg.
- Avouris, P. (2002). Carbon nanotube electronics. *Chemical Physics*, Vol. 281, No. 2-3, (March 2002), pp. (429-445), ISSN 0301-0104.
- Back, J.H., Shim, M. (2006). pH-dependent electron-transport properties of carbon nanotubes. *Journal of Physical Chemistry B*, Vol. 110, (October 2006), pp. (23736-23741), ISSN 1089-5647.
- Bordjiba, T., Mohamedi, M., & Dao, L.H. (2008). Charge storage mechanism of binderless nanocomposite electrodes formed by dispersion of CNTs and carbon aerogels. *Journal of the Electrochemical Society*, Vol. 155, No. 2, (December 2007), pp. (A115-A124), ISSN 0013-4651.
- Centeno, T.A., Hahn, M., Fernández, J.A., Kötz, R., & Stoeckli, F. (2007). Correlation between capacitances of porous carbons in acidic and aprotic EDLC electrolytes. *Electrochemistry Communications*, Vol. 9, No. 6, (June 2007), pp. (1242-1246), ISSN 1388-2481.
- Chaban, V.V., Kalugin, O.N. (2009). Structure and Dynamics in Methanol and its Lithium Ion Solution Confined by Carbon Nanotubes. *Journal of Molecular Liquids*, Vol. 145, No. 3, (May 2009), pp. (145-151), ISSN 0167-7322.
- Chaban, V.V., Kalugin, O.N. (2010). Liquid dimethyl sulphoxide confined by carbon nanotubes. *Journal of Molecular Liquids*, Vol. 151, No. 2-3, (February 2010), pp. (113-116), ISSN 0167-7322.
- Chaban, V.V., Kalugin, O.N., Habenicht, B.F., & Prezhdov, O.V. (2010). The Influence of the Rigidity of a Carbon Nanotube on the Structure and Dynamics of Confined Methanol. *Journal of the Physical Society of Japan*, Vol. 79, No. 6, (June 2010), pp. (064608.1-064608.5), ISSN 1347-4073.
- Convert, P., Coutanceau, C., Crouigneau, P., Gloaguen, F., & Lamy, C. (2001). Electrodes modified by electrodeposition of CoTAA complexes as selective oxygen cathodes in a direct methanol fuel cell. *Journal of Applied Electrochemistry*, Vol. 31, No. 9, (September 2001), pp. (945-952), ISSN 0021-891X.

- Danilov, M.O., Melezhik, A.V., & Danilenko, N.I. (2005). Carbon nanotubes as catalyst supports for oxygen electrodes. *Russian Journal of Applied Chemistry*, Vol. 78, No. 11, (November 2005), pp. (1849-1853), ISSN 1070-4272.
- Eletsii, A.V. (1997). Carbon nanotubes. *Uspekhi Fizicheskikh Nauk*, Vol. 167, No. 9, (September 2005), pp. (945-972), ISSN 1996-6652.
- Endo, M., Strano, M.S., & Ajayan, P.M. (2008). Potential applications of carbon nanotubes, In: *Carbon Nanotubes, Topics in Applied Physics, Vol. 111*, A. Jorio, G. Dresselhaus, M. S. Dresselhaus (Eds.), pp. (13-62), Springer, ISBN 978-3-540-72864-1, Berlin, Heidelberg.
- Gu, Y.J., Wong, W.T. (2006). Nanostructure PtRu/MWNTs as anode catalysts prepared in a vacuum for direct methanol oxidation. *Langmuir*, Vol. 22, No. 26, (November 2006), pp. (11447-11452), ISSN 0743-7463.
- Haughney, M., Ferrario, M., & McDonald, I.R. (1987). Molecular-dynamics simulation of liquid methanol. *Journal of Physical Chemistry*, Vol. 91, No. 19, (September 1987), pp. (4934-4940), ISSN 0022-3654.
- Hilder, T.A., Hill, J.M. (2008). Carbon nanotubes as drug delivery nanocapsules. *Current Applied Physics*, Vol. 8, No. 3-4, (May 2008), pp. (258-261), ISSN 1567-1739.
- Hsieh, C.T., Lin, J.Y. (2009). Fabrication of bimetallic Pt-M (M = Fe, Co, and Ni) nanoparticle/carbon nanotube electrocatalysts for direct methanol fuel cells. *Journal of Power Sources*, Vol. 188, No. 2, (March 2009), pp. (347-352), ISSN 0378-7753.
- Hsieh, C.T., Lin, J.Y., & Yang, S.Y. (2009). Carbon nanotubes embedded with PtRu nanoparticles as methanol fuel cell electrocatalysts. *Physica E-Low-Dimensional Systems & Nanostructures*, Vol. 41, No. 3, (January 2009), pp. (373-378), ISSN 1386-9477.
- Huang, J.S., Sumpster, B.G., & Meunier, V. (2008). A universal model for nanoporous carbon supercapacitors applicable to diverse pore regimes, carbon materials, and electrolytes. *Chemistry-A European Journal*, Vol. 14, No. 22, (July 2008), pp. (6614-6626), ISSN 0947-6539.
- Huang, C.W., Chuang, C.M., Ting, J.M., & Teng, H.S. (2008). Significantly enhanced charge conduction in electric double layer capacitors using carbon nanotube-grafted activated carbon electrodes. *Journal of Power Sources*, Vol. 183, No. 1, (August 2008), pp. (406-410), ISSN 0378-7753.
- Janes, A., Kurig, H., & Lust, E. (2007). Characterisation of activated nanoporous carbon for supercapacitor electrode materials. *Carbon*, Vol. 45, No. 6, (February 2007), pp. (1226-1233), ISSN 0008-6223.
- Kalugin, O.N., Adya, A.K., Volobuev, M.N., & Kolesnik, Ya.V. (2003). Solvation of solvophilic and solvophobic ions in dimethyl sulphoxide: microscopic structure by molecular dynamics simulations. *Physical Chemistry Chemical Physics*, Vol. 5, No. 8, (March 2003), pp. (1536-1546), ISSN 1463-9076.
- Kalugin, O.N., Pazura, Yu.I., & Kolesnik, Ya.V. (2005). Internal structure of tetraalkylammonium ions in infinitely diluted solutions in acetonitrile, dimethyl sulphoxide and methanol. *Kharkiv University Bulletin*, Vol. 669, No. 13(36), pp. (162-168), ISSN 0453-8048.
- Kalugin, O.N., Chaban, V.V., & Kolesnik, Y.V. (2006). Molecular dynamics simulation of liquid acetonitrile and solution of Li<sup>+</sup> in it inside carbon nanotubes by using

- MDCNT package. *Kharkov University Bulletin*, Vol. 731. Chemical Series, No. 14(37), (December 2006), pp. (41-58), ISSN 0453-8048.
- Kalugin, O.N., Chaban, V.V., Loskutov, V.V., & Prezhdo, O.V. (2008). Uniform Diffusion of Acetonitrile inside Carbon Nanotubes Favors Supercapacitor Performance. *Nano Letters*, Vol. 8, No. 8, (July 2008), pp. (2126-2130), ISSN 1530-6984.
- Li, W.Z., Liang, C.H., & Xin, Q. (2004). Application of novel carbon nanomaterials in low-temperature fuel cell catalysts. *Chinese Journal of Catalysis*, Vol. 25, No. 10, (October 2004), pp. (839-843), ISSN 1872-2067.
- Lin, M.L., Huang, C.C., Lo, M.Y., & Mou, C.Y. (2008). Well-ordered mesoporous carbon thin film with perpendicular channels: Application to direct methanol fuel cell. *Journal of Physical Chemistry C*, Vol. 112, (January 2008), pp. (867-873), ISSN 1932-7447.
- Lin, R., Taberna, P.L., Chmiola, J., Guay, D., Goqotsi, Y., & Simon, P. (2009). Microelectrode Study of Pore Size, Ion Size, and Solvent Effects on the Charge/Discharge Behavior of Microporous Carbons for Electrical Double-Layer Capacitors. *Journal of the Electrochemical Society*, Vol. 156, No. 1, (October 2008), pp. (A7-A12), ISSN 0013-4651.
- Liu, H., Muller-Plathe, F., van Gunsteren, W.F. (1995). A force field for liquid dimethyl sulfoxide and physical properties of liquid dimethyl sulfoxide calculated using molecular dynamics simulation. *Journal of American Chemical Society*, Vol. 117, No. 15, (April 1995), pp. (4363-4366), ISSN 0002-7863.
- Liu, H.S., Song, C.J., Zhang, L., Zhang, J., Wang, H., & Wilkinson, D.P. (2006). A review of anode catalysis in the direct methanol fuel cell. *Journal of Power Sources*, Vol. 155, No. 2, (April 2006), pp. (95-110), ISSN 0378-7753.
- Liu, Z., Chen, K., Davis, C., Sherlock, S., Cao, Q., Chen, X., & Dai, H. (2008). Drug delivery with carbon nanotubes for in vivo cancer treatment. *Cancer Research*, Vol. 68, No. 16, (August 2008), pp. (6652-6660), ISSN 0008-5472.
- Maclean, H.L., Lave, L.B. (2003). Evaluating automobile fuel/propulsion system technologies. *Progress in Energy and Combustion Science*, Vol. 29, No. 1, (February 2003), pp. (1-69), ISSN 0360-1285.
- Martin, D., Hanthall, H.G. (1975). *Dimethyl Sulfoxide*, Wiley, New York.
- Mountain, R.D. (1997). Shear viscosity and dielectric constant of liquid acetonitrile: A computer simulation study. *Journal of Chemical Physics*, Vol. 107, No. 10, (September 1997), pp. (3921-3923), ISSN 0021-9606.
- Peng, Z., Ewig, C.S., Hwang, H.-J., Waldman, M., & Hagler, A.T. (1997). Derivation of Class II Force Fields. 4. van der Waals Parameters of Alkali Metal Cations and Halide Anions. *Journal of Physical Chemistry A*, Vol. 107, No. 39, (September 1997), pp. (7243-7252), ISSN 1089-5639.
- Poltoratchkij, G.M. (1984). *Thermodynamic characteristics of non-aqueous electrolyte solutions. Handbook*, Chemistry, Leningrad, USSR
- Qi, L., Xie, X.F., Xu, J.M., & Zhou, Q.F. (2006). Transport phenomena and numerical simulation related to water in direct methanol fuel cell. *Progress in Chemistry*, Vol. 18, No. 012, (December 2006), pp. (1725-1734), ISSN 1005281X.
- Schultz, T., Zhou, S., & Sundmacher, K. (2001). Current status of and recent developments in the direct methanol fuel cell. *Chemical Engineering & Technology*, Vol. 24, No. 12, (December 2001), pp. (1223-1233), ISSN 0930-7516.

- Sevriugin, V.A., Loskutov, V.V., & Skirda, V.D. (2003). Dependence of the self-diffusion coefficient of liquid molecules in a porous medium on its geometric parameters. *Colloid Journal*, Vol. 65, No. 5, (September 2003), pp. (602-605), ISSN 1061-933X.
- Suffredini, H.B., Salazar-Banda, G.R., & Avaca, L.A. (2009). Carbon supported electrocatalysts prepared by the sol-gel method and their utilization for the oxidation of methanol in acid media. *Journal of Sol-Gel Science and Technology*, Vol. 49, No. 2, (November 2008), pp. (131-136), ISSN 0928-0707.
- Van Gunsteren, W.F., Billeter, S.R., Eising, A.A., Hünenberger, P.H., Kürger, P., Mark, A.E., Scott, W.R.P. & Tironi, I.G. (1996). *Biomolecular Simulation: The GROMOS 96 Manual and User Guide*. Zürich Biomos b.v. ISBN 3 7281 2422 2, Zürich, Groningen.
- Wang, C.H., Dub, H.Y., Tsai, Y.T., Chen, C.-P., Huang, C.-J., Chen, L.C., Chen, K.H., & Shin, H.-C. (2007). High performance of low electrocatalysts loading on CNT directly grown on carbon cloth for DMFC. *Journal of Power Sources*, Vol. 171, No. 1, (September 2007), pp. (55-62), ISSN 0378-7753.
- Wang, Z., Zhu, Z.Z., Li, Y.X., & Li, H.L. (2008). Highly dispersed palladium nanoparticles on functional MWNT surfaces for methanol oxidation in alkaline solutions. *Chinese Journal of Chemistry*, Vol. 26, No. 4, (April 2008), pp. (666-670), ISSN 1614-7065.
- Wu, F., Xu, B. (2006). Progress on the application of carbon nanotubes in supercapacitors. *New Carbon Materials*, Vol. 21, No. 2, (June 2006), pp. (176-184), ISSN 1872-5805.
- Yang, F., Fu, D., Long, J., & Ni, Q.X. (2008). Magnetic lymphatic targeting drug delivery system using carbon nanotubes. *Medical Hypotheses*, Vol. 70, No. 4, (October 2007), pp. (765-767), ISSN 0306-9877.
- Yang, X., Zhang, Z., Liu, Z., Ma, Y., Yang, R., & Chen, Y. (2008). Multi-functionalized single-walled carbon nanotubes as tumor cell targeting biological transporters. *Journal of Nanoparticle Research*, Vol. 10, No. 5, (November 2007), pp. (815-822), ISSN 1388-0764.
- Yu, Z.W., Quinn, P.J. (1994). Dimethyl-Sulfoxide - a Review of Its Applications in Cell Biology. *Bioscience Reports*, Vol. 14, No. 6, (December 1994), pp. (259-281), ISSN 0144-8463.
- Yu, Z.W., Quinn, P.J. (1998). The modulation of membrane structure and stability by dimethyl sulphoxide (Review). *Molecular Membrane Biology*, Vol. 15, No. 1, (January 1998), pp. (59-68), ISSN 0968-7688.
- Zhang, R., Baxendale, M., & Peijs, T. (2007). Universal resistivity-strain dependence of carbon nanotube/polymer composites. *Physical Review B*, Vol. 76, No. 19, (November, 2007), pp. (195433.1-195433.5), ISSN 1098-0121.



## **Carbon Nanotubes - Synthesis, Characterization, Applications**

Edited by Dr. Siva Yellampalli

ISBN 978-953-307-497-9

Hard cover, 514 pages

**Publisher** InTech

**Published online** 20, July, 2011

**Published in print edition** July, 2011

Carbon nanotubes are one of the most intriguing new materials with extraordinary properties being discovered in the last decade. The unique structure of carbon nanotubes provides nanotubes with extraordinary mechanical and electrical properties. The outstanding properties that these materials possess have opened new interesting researches areas in nanoscience and nanotechnology. Although nanotubes are very promising in a wide variety of fields, application of individual nanotubes for large scale production has been limited. The main roadblocks, which hinder its use, are limited understanding of its synthesis and electrical properties which lead to difficulty in structure control, existence of impurities, and poor processability. This book makes an attempt to provide indepth study and analysis of various synthesis methods, processing techniques and characterization of carbon nanotubes that will lead to the increased applications of carbon nanotubes.

### **How to reference**

In order to correctly reference this scholarly work, feel free to copy and paste the following:

Oleg N. Kalugin, Vitaly V. Chaban and Oleg V. Prezhdo (2011). Microscopic Structure and Dynamics of Molecular Liquids and Electrolyte Solutions Confined by Carbon Nanotubes: Molecular Dynamics Simulations, Carbon Nanotubes - Synthesis, Characterization, Applications, Dr. Siva Yellampalli (Ed.), ISBN: 978-953-307-497-9, InTech, Available from: <http://www.intechopen.com/books/carbon-nanotubes-synthesis-characterization-applications/microscopic-structure-and-dynamics-of-molecular-liquids-and-electrolyte-solutions-confined-by-carbon>

**INTECH**  
open science | open minds

### **InTech Europe**

University Campus STeP Ri  
Slavka Krautzeka 83/A  
51000 Rijeka, Croatia  
Phone: +385 (51) 770 447  
Fax: +385 (51) 686 166  
[www.intechopen.com](http://www.intechopen.com)

### **InTech China**

Unit 405, Office Block, Hotel Equatorial Shanghai  
No.65, Yan An Road (West), Shanghai, 200040, China  
中国上海市延安西路65号上海国际贵都大饭店办公楼405单元  
Phone: +86-21-62489820  
Fax: +86-21-62489821

© 2011 The Author(s). Licensee IntechOpen. This chapter is distributed under the terms of the [Creative Commons Attribution-NonCommercial-ShareAlike-3.0 License](#), which permits use, distribution and reproduction for non-commercial purposes, provided the original is properly cited and derivative works building on this content are distributed under the same license.

IntechOpen

IntechOpen